Cavitation Modelling

Y. Meslem[†] , S. Honnet[‡], W. Schwarz[⋇], J. Reveillon[†] and F.X. Demoulin[†]

[†]UMR6614-CORIA, Technopole du Madrillet, BP 12, Avenue de l'Universite, 76801 Saint-Etienne-du-Rouvray Cedex, France
[‡]PSA Peugeot Citroen, Centre Technique de Velizy, Route de Gisy 78943 Velizy-Villacoublay, France
[⋇] AVL France, 2-4 rue Hans List F-78290 Croissy sur Seine, France
yann.meslem@coria.fr and demoulin@coria.fr

Abstract

Strong local pressure drops have been observed in many Diesel injectors and as a result, cavitation occurs. Some studies have shown that the occurrence of this phenomenon modifies basic characteristics of the spray. Cavitation models are based on the dynamics of spherical vapor bubbles, expressed by the well-known Rayleigh-Plesset equation. However, in cavitating zones, bubbles coalescence forms gaseous cavities. These cavities are stretched by the liquid flow and can not be considered as spherical elements anymore. The presented cavitation model accounts for this observation in cavitating flows. The model is designed with the Eulerian-Lagrangian for Spray and Atomization model (ELSA) framework of Vallet and Borghi [10]. A particular care is taken to deal with reference conditions of cavitation nuclei, that is to say for pressure and size of the nuclei before cavitation occurrence. A real injector configuration is chosen as test case.

Introduction

During the last decade, the combustion efficiency in Diesel engines has risen by the improvement of injection systems. The increase of injection pressure has been one of the main strategies to reach that goal. Nevertheless, strong local pressure drops have been observed in many Diesel injectors and as a result, cavitation occurs. According to He and Ruiz [5] the dense zone of the spray is influenced by the in-injector flow and particularly by the cavitation phenomenon. On the one hand, Tamaki *et al* [9] established that great turbulence in the nozzle hole, induced by cavitation, contributes greatly to the disintegration of the liquid jet, improving the atomization process. On the other hand, Payri *et al* [8] and Andriotis *et al* [1] have respectively determined that an increment of spray angle is associated with string cavitation inside the nozzle sac and that cavitation affects the spray penetration. In other words, the occurrence of cavitation modifies basic characteristics of the spray which play a major role in the Diesel combustion.

Computational Methods

Overview of the Eulerian-Lagrangian Spray Atomization model: basic equations

The coarse point to quantify the contribution of cavitation on the atomization processes consists in relating the cavitating flow inside the injector to the spray formation in the combustion chamber. The main problem is to describe the dense zone at the injector exit. That can be done directly thanks to the Eulerian-Lagrangian for Spray and Atomization (ELSA) model implemented in the solver AVL FIRE. As this model can also be used to simulate in-injectors flows, it is a good model to study impact of cavitation on atomization processes. That is why it has been developped to be able to consider cavitation phenomenon. Here is an overview of the ELSA model.

This model was designed originally by Vallet and Borghi ([10], [11] and developped by Lebas *et al* [6]) to describe atomization of flows with high Weber and Reynolds values. Its distinctive feature is to consider the dense zone of the spray with an Eulerian approach, considering that this approach is more adapted to describe strong interactions between phases.

Principle of an Eulerian approach is to consider the two phase flow as a single phase flow composed of two species, liquid and gas, with highly variable density $\bar{\rho}$. Consequently, there is only one velocity for the two phases mixing. It should be noted that further work have been done by Blokkeel *et al* [2] to couple the Eulerian approach in the dense zone with the Lagrangian approach in the diluted one. However, the focus is on the dense zone and this part of the model will not be described in this paper.

⋇Corresponding author: yann.meslem@coria.fr

To begin with, mass weighted Favre average is used for ELSA model variables. Considering a variable A, its Reynolds average is noted $\bar{A}$ and the corresponding fluctuation is noted A'. The mass weighted Favre average is $\widetilde{A}$ and the corresponding fluctuation is noted A''. Here is the calculation of the mass weighted Favre average of A:

$$\begin{cases} \rho = \bar{\rho} + \rho' \\ A = \widetilde{A} + A'' \quad \text{with} \quad \bar{\rho}\widetilde{A} = \rho\bar{A} \end{cases} \tag{1}$$

Thus, in the ELSA model, $\bar{\rho}$ represents the mean mixture density, $\widetilde{u}$ is the Favre averaged mixture velocity and $\bar{p}$ is the mean pressure. The model solves that mean mixture velocity using standard k-ε equations, written in their standard single flow formalism without modification. Indeed, in spite of the fact that those equations have been developed in a single flow formalism, Demoulin *et al* [3] have shown that this standard model is able to reproduce the main characteristics of the two phase flow if special care is devoted to the modelling of the turbulent mass flux.

Both liquid mass fraction $\widetilde{Y}_l$ and liquid volume fraction $\bar{\Phi}_l$ are implemented in the model. These variables are linked by the following equation:

$$\widetilde{Y}_l = \frac{\rho_l \bar{\Phi}_l}{\bar{\rho}} \tag{2}$$

The mean mixture density $\bar{\rho}$ depends on liquid volume fraction and liquid and gas densities:

$$\frac{1}{\bar{\rho}} = \frac{\widetilde{Y}_l}{\rho_l} + \frac{1-\widetilde{Y}_l}{\rho_g} \tag{3}$$

Transport equation of liquid mass fraction is given below:

$$\frac{\partial \bar{\rho}\widetilde{Y}_l}{\partial t} + \frac{\partial \bar{\rho}\widetilde{U}_j\widetilde{Y}_l}{\partial x_j} = -\frac{\partial \bar{\rho}\widetilde{U_j''Y_l''}}{\partial x_j} - \bar{\rho}\dot{m}_{vap}\widetilde{\Omega} \tag{4}$$

In this equation, $\widetilde{U}_j$ is the component of mean liquid/gas velocity for "j" direction. The second term of the right hand side concerns the vaporization: the model is based on a classical D^2's law. This equation contains only one unclosed term: $\widetilde{U_j''Y_l''}$. It is namely the turbulent liquid flux and it can be noted R_{jY_l} . For turbulent single phase flows, the gradient closure approximation is generally applied:

$$\widetilde{U_j''Y_l''} = R_{jY_l} = -\frac{\mu_t}{Sc_t}\frac{\partial \widetilde{Y}_l}{\partial x_j} \tag{5}$$

ν_t is a turbulent viscosity coefficient whereas Sc_t is a turbulent Schmidt number. This term is important because it represents the liquid dispersion due to turbulent fluctuations. It can also represent the mean slip between the phases. Because the phases are strictly separated, it is possible to derive the exact following relation (Demoulin *et al* [3]):

$$\widetilde{U_j''Y_l''} = \widetilde{Y}_l(1-\widetilde{Y}_l)(\overline{u_{\widetilde{Y}_l,j}|_l} - \overline{u_{\widetilde{Y}_l,j}|_g}) = \widetilde{Y}(\overline{u_{\widetilde{Y}_l,j}|_l} - \widetilde{U}_j) \tag{6}$$

where $\bar{u}_{\widetilde{Y}_l,j}|_l$ and $\bar{u}_{\widetilde{Y}_l,j}|_g$ are mean velocities conditioned respectively by liquid and gas phases.

An additional equation has been added for the liquid/gas interface density $\bar{\Sigma}$ (m^{-1}). It is the quantity of liquid/gas interface per unit of volume. The quantity of liquid/gas interface per unit of mass is rather used to simplify the equation and more especially the treatment of the diffusive term. It is defined by:

$$\widetilde{\Omega} = \frac{\bar{\Sigma}}{\bar{\rho}} \tag{7}$$

This equation, originally proposed by Vallet and Borghi [10] was postulated by analogy with the transport equation of the flame surface density of Marble and Broadwell [7]. The first interest of this equation is to avoid any

assumption concerning the shape of the liquid surface, especially the assumption of spherical droplets, and try to describe realistically this two phase flow. The transport equation is assumed as follows:

$$\frac{\partial \bar{\rho}\widetilde{\Omega}}{\partial t} + \frac{\partial \bar{\rho}\widetilde{U}_j\widetilde{\Omega}}{\partial x_j} = -\frac{\partial \bar{\rho}\widetilde{U_j''\Omega''}}{\partial x_j} + \sum_i \bar{\rho}\dot{\widetilde{\Omega}}_i \ . \tag{8}$$

All the $\dot{\widetilde{\Omega}}_i$ terms represents source terms to consider processus acting on interface production or destruction, as vaporization, coalescence, break-up phenomenon. The production by turbulent mixing between liquid and gas and mean shear stress are also taken into account. The first term of the right hand side is unclosed since it requires the mean surface velocity. A turbulent diffusive term can model it in the framework of atomization process approaches.

In the end, Eulerian and Lagrangian approaches can be linked in the diluted zone but this part of the ELSA model will not be discussed in the present article.

Cavitation modelling

Cavitation model is based on the Rayleigh-Plesset equation. Bubble radius is calculated depending on flow conditions and fluid properties. However, to be able to consider gas cavities and not only spherical bubbles, the model must be able to free oneself from bubble radius. A characteristic length called L_{32} is defined, depending on liquid and gas volume fractions and surface quantity and replaces bubble radius in source terms. This characteristic length is not the solved variable. Surface density and liquid and gas fractions are the solved ones in the model. The characteristic length is then calculated according to the previously mentioned solved variables. By this way, the cavitation model is able to deal with non spherical gaseous cavities.

$$L_{32} = \frac{3\bar{\Phi}_l\bar{\Phi}_g}{\bar{\Sigma}} \tag{9}$$

Bubble number density can also be expressed according to volume fractions and surface quantity, as shown in the following equation. To begin, the model does not take into account for variable nucleation rate. Bubble number density is calculated with equation (10) to check if variations of surface density and liquid and gas fractions are coherent.

$$N_b = \frac{\bar{\Sigma}^3}{36\pi\left(\bar{\Phi}_l\bar{\Phi}_g\right)^2} \tag{10}$$

In the same way as the characteristic length L_{32}, interface velocity $\widetilde{U_i}$ is rather used instead of bubble growing velocity $\dot{R}$. Characteristic time τ_{cavit} is defined according to the interface velocity $\widetilde{U_i}$ and characteristic length L_{32}:

$$\tau_{cavit} = \frac{L_{32}}{\widetilde{U_i}} \tag{11}$$

Transport of the interface velocity $\widetilde{U_i}$ is an innovative feature of this model. It can be noted that both liquid and gas fractions have to be transported and solved in order to keep accuracy. Then, major specie calculation is based on the minor one to keep mass conservation. Source terms from cavitation occurrence which appear in mass conservation equations for gas and liquid mass fraction and in surface density equation are respectively given by equations (12), (13) and (14):

$$\frac{\partial \bar{\rho}\widetilde{Y}_g}{\partial t}\|_{cavit} = 3\bar{\rho}\widetilde{Y}_g\frac{1}{\tau_{cavit}}\bar{\Phi}_l \tag{12}$$

$$\frac{\partial \bar{\rho}\widetilde{Y}_l}{\partial t}\|_{cavit} = -3\bar{\rho}\widetilde{Y}_l\frac{1}{\tau_{cavit}}\bar{\Phi}_g \tag{13}$$

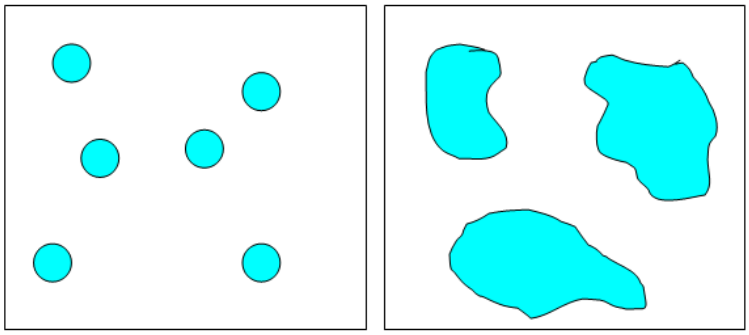

Figure 1. Cavitation nuclei are represented on the left. After a pressure drop, these cavitation nuclei grow to become bubbles and then gaseous cavities.

$$\frac{\partial \bar{\rho}\widetilde{\Omega}}{\partial t}\|_{cavit} = 2\bar{\rho}\widetilde{\Omega}\frac{1}{\tau_{cavit}}\left(\bar{\Phi}_l - \bar{\Phi}_g\right) \tag{14}$$

Most of modelling work concerns interface velocity. Source terms are partially given by the Rayleigh-Plesset equation (15), where σ and μ_l are respectively the surface tension coefficient and liquid dynamic viscosity. R is bubble radius as this equation rules spherical bubble dynamics. P_b is the pressure inside the bubble (detailed in the next section) and P_∞ is the pressure far away from the bubble.

$$\rho_l\left(R\ddot{R} + \frac{3}{2}\dot{R}^2\right) = P_b - P_\infty - \frac{2\sigma}{R} - 4\mu_l\frac{\dot{R}}{R} \tag{15}$$

The quantity of interface velocity is transported, that is to say $\bar{\Sigma}\widetilde{U_i}$ and not only $\widetilde{U_i}$. Consequently, its variation depends both on surface density variation and on flow conditions (local pressure):

$$\frac{\partial \bar{\rho}\widetilde{\Omega}\widetilde{U_i}}{\partial t}\|_{cavit} = \widetilde{U_i}\frac{\partial \bar{\rho}\widetilde{\Omega}}{\partial t} + \bar{\Sigma}\frac{\partial \widetilde{U_i}}{\partial t} \tag{16}$$

First term of the right-hand side depends on source terms for surface density (cf. end of the first section). In the framework of in-injectors flow, among the different mentioned phenomena which can be taken into account for surface density variations, only terms for relevant phenomena are used. For instance, term for surface density variation depending on droplet breakup is obviously ignored. Concerning the second term of the right-hand side, two cases need to be distinguished: when there is almost only liquid, cavitation nuclei can be assumed to be spherical and therefore Rayleigh-Plesset equation (15) is used to calculate the last term of the previous equation.

When gas volume fraction exceed a threshold value, source terms corresponding to a dense zone modelling are used. An illustration of what is called dense zone is shown on Figure 1. The threshold value is equal to 0.1 but could be reviewed. Modelling proposal in the dense zone is shown in the equation (17).

$$\frac{\partial \widetilde{U_i}}{\partial t} = \bar{\Sigma}\frac{(P_{sat} - P_\infty)}{\rho_l} \tag{17}$$

This modelling proposal is close to the term using Rayleigh-Plesset equation. Only driving pressure term is kept. Indeed, the other terms are linked to bubble sphericity assumption and lose their sense in case of larger gaseous structure or are hard to estimate. Term for surface tension effects enters in the second category as the gaseous structure curvature is hard to estimate. It can be noted that saturation pressure is used in the driving pressure term instead of general bubble pressure. This last pressure is the sum of residual gas partial pressure (pressure in cavitation nuclei before cavitation occurrence) and vapor partial pressure after nuclei growing, as illustrated by the Figure 2.

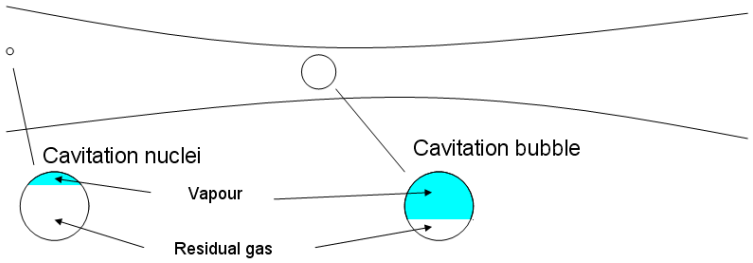

Figure 2. In case of pressure drop, cavitation nuclei grow to become bubbles. Gas pressure ratio between residual gas partial pressure and vapor partial pressure is modified. Pressure inside the bubble tends to saturation pressure when bubbles go on growing.

$$\text{If } \left(\bar{\Phi}_g \leq 0.1\right) :$$

$$\frac{\partial \bar{\Sigma}\widetilde{U_i}}{\partial t}\|_{cavit} = 2\bar{\Sigma}\widetilde{U_i}\frac{1}{\tau_{cavit}}\left(\bar{\Phi}_l - \bar{\Phi}_g\right) + \frac{\bar{\Sigma}}{L_{32}}\left(\frac{\Delta P}{\rho_l} - \frac{3}{2}\widetilde{U_i}^2 - 4\nu_l\frac{\widetilde{U_i}}{L_{32}}\right) \tag{18}$$

$$\text{If } \left(\bar{\Phi}_g > 0.1\right) :$$

$$\frac{\partial \bar{\Sigma}\widetilde{U_i}}{\partial t}\|_{cavit} = 2\bar{\Sigma}\widetilde{U_i}\frac{1}{\tau_{cavit}}\left(\bar{\Phi}_l - \bar{\Phi}_g\right) + \bar{\Sigma}\frac{(P_{sat} - P_\infty)}{\rho_l} \tag{19}$$

With: $\Delta P = P_b - P_\infty - \dfrac{2\sigma}{L_{32}}$

When bubbles grow to become larger gaseous structures, the part of residual gas is very small and pressure inside the gaseous structure can be estimate to saturation pressure P_{sat}. Source terms used according to flow conditions and composition of the mixture are sum up above.

Reference conditions issue

Cavitation models generally need nuclei for cavitation inception. We will see in this section (based on work of Franc [4]) that the choice of nuclei's caracteristics (pressure of residual gas and radius) can influence significantly results of the model. A bubble is in equilibrium when the following equation is respected. P_{rg} is residual gas pressure. It depends on bubble radius R, nucleus radius R_0 and nucleus pressure $P_{rg,0}$ and can be estimated using the ideal gas law. Indeed, it is common to assume the gas transformation as isothermal since the temperature can be considered as continuously fixed by temperature of the liquid.

$$\begin{aligned} P_b &= P_\infty + \frac{2\sigma}{R} \\ \text{As } P_b &= P_{rg} + P_{sat} \\ \text{and } P_{rg} &= P_{rg,0}\left(\frac{R_0}{R}\right)^3 \\ P_\infty &= P_{rg,0}\left(\frac{R_0}{R}\right)^3 + P_{sat} - \frac{2\sigma}{R} \end{aligned} \tag{20}$$

By solving this equation with respect to R, a radius of equilibrium of a bubble can be obtained at any external pressure P_∞, as shown on the Figure 3. It can be noted that equilibrium is not always stable. Thus, two critical values (equations (21) for critical radius R_c and (22) for critical pressure P_c) can be expressed according to what is called here reference conditions, that is to say according to pressure and radius of the nucleus $P_{rg,0}$ and R_0.

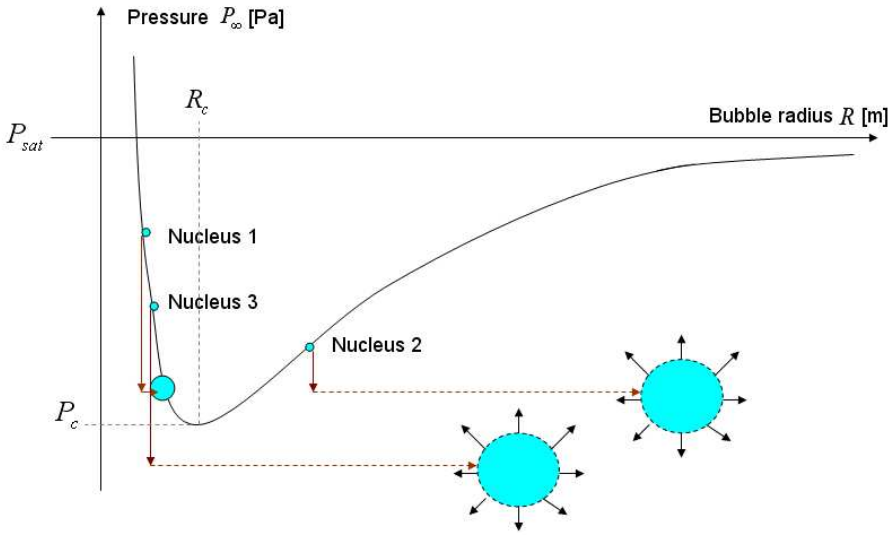

Figure 3. Equilibrium radius of a cavitation nucleus depending on pressure far away in the liquid. Illustration of the behaviour of three nuclei of different initial radius in case of pressure drop.

$$R_c = \sqrt{\frac{3P_{rg,0}R_0^3}{2\sigma}} \tag{21}$$

$$P_c = P_{sat} - \frac{2}{3}\frac{2\sigma}{R_c} \tag{22}$$

Nuclei will grow with different behaviours if their initial radius R_0 is different. Three examples are illustrated on the Figure 3. Radius of nuclei 1 and 3 is smaller than critical radius whereas radius of nucleus 2 is bigger. For the same pressure drop, Nucleus 1 will reach a stable equilibrium because the new pressure stays higher than the critical pressure. Nucleus 2 will be subjected to unlimited growth because new pressure is lower than critical pressure which corresponds to the minimum of the equilibrium curve. Eventually, nucleus 3 will be subjected to unlimited growth too because its initial radius was higher than critical radius: it was initially in an unstable equilibrium.

The threshold pressure for cavitation occurrence is generally considered as vapor pressure but the Figure 3 illustrates clearly that the threshold pressure is actually the nucleus critical pressure P_c. Equation (22) shows critical pressure is lower than saturation pressure. Difference is due to surface tension which depends on nucleus radius. A nucleus can be characterized by its critical radius and pressure. Consequently, results of cavitation models depends on nuclei characteristics. Unfortunately only little information exist on nuclei and it is very hard to find order of magnitude for its radius or the pressure they are considered to exist.

In order to improve this aspect of the modelling for cavitating flow calculations, a methodology has been setted up. The first step is to identify two zones, "pre-cavitating zone" and cavitating zone, on a first calculation without cavitation modelling. The "pre-cavitating zone" is the zone usptream the cavitating zone and the zone where nuclei are considered to exist. The aim is to know order of magnitude of pressure in the pre-cavitating and in the cavitating zones in order to set the reference conditions. That last step can be done studying equilibrium curves as in the Figure 3 with different couples of value (P_0, R_0). Reference conditions are chosen according to comparisons between critical values (P_c, R_c) and order of magnitude of pressure for the two zones. P_0 must be closed to the pre-cavitating zone pressure and P_c must exceed pressure of the cavitating zone but must also be lower than the lowest pressure level in the precavitating zone. Eventually, R_0 must be smaller than R_c and has to be chosen for nuclei to have the behaviour of the Nucleus 3.

Results and Discussion

Tests which have been done in this part are based on data extracted from a 3D simulation with the CFD solver AVL Fire. A real injector have been meshed to simulate the in-injector flow. Then, an interesting streamline

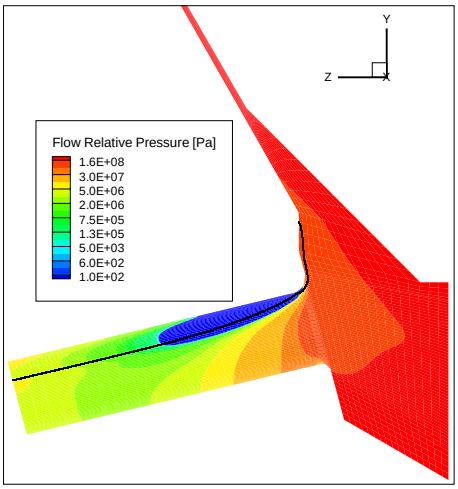

Figure 4. Bubble Streamline extracted from a 3D calculation and selected for the case with pressure field.

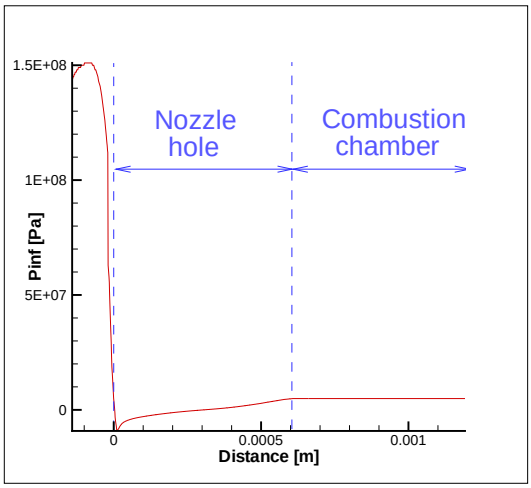

Figure 5. Pressure history along the streamline.

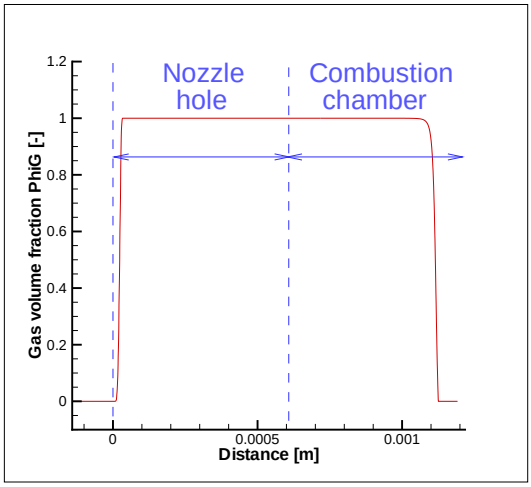

Figure 6. Variation of gas volume fraction along the streamline.

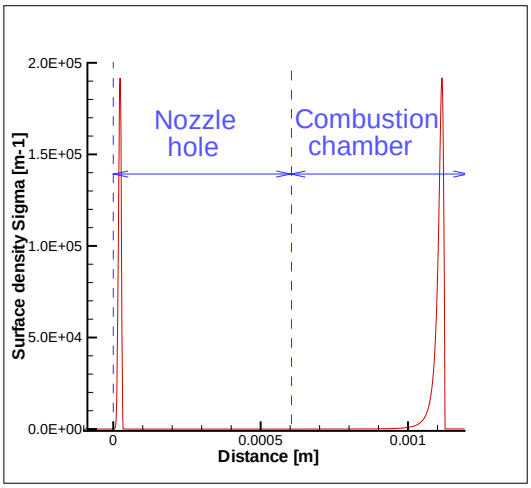

Figure 7. Maxima of surface density corresponds to equi-distribution between liquid and gas.

has been selected in order to follow a bubble trajectory and to be able to extract and use realistic data for the tests. Figure 4 shows pressure field in the injector hole and the pressure in the combustion chamber. Distance variable corresponds to the distance travelled by the bubble along the followed streamline. Results are hopeful for calculations in the previously described dense zones configurations. Response to the pressure drop from gas volume fraction and surface density looks reasonably good on the Figures 6 and 7. Surface density response is the one expected, with maxima reached for equi-distribution between liquid and gas. Figure 8 illustrates the good transition between source term from classical Rayleigh-Plesset equation and the modelling proposed for the dense zone. Of course, comparisons between calculations with the model and experimental results will be necessary for its validation. They will be shown during the oral presentation.

Summary and Conclusions

A cavitation model has been presented. The main advantage of this model is to be abble to deal with non spherical gaseous structures, like huge gaseous cavities in Diesel injectors. A distinctive feature of the model is to transport interface velocity in order to keep second order time derivative of the bubble radius in the Rayleigh-Plesset equation so as to improve accuracy. Reference conditions issue for cavitation nuclei, that is to say estimation of residual gas pressure and radius of the nuclei, has been raised and a procedure has been proposed. Eventually, first

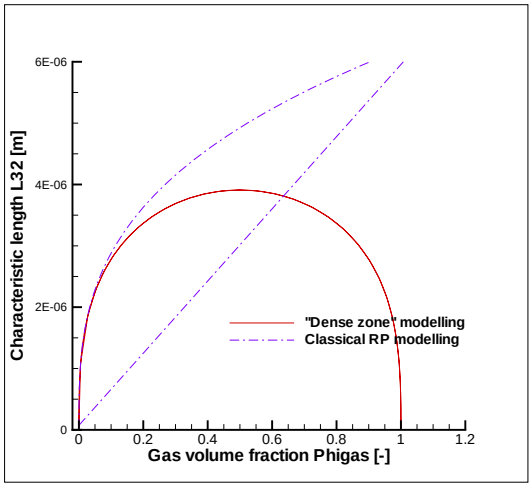

Figure 8. Variation of L_{32} according to gas volume fraction.

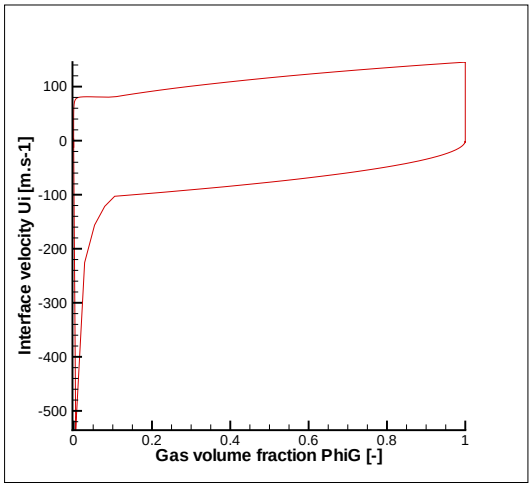

Figure 9. Variation of interface velocity U_i according to gas volume fraction.

results of the model has been presented. Calculations are based on pressure history extracted from a 3D calculation with the CFD solver AVL Fire along a bubble streamline. Results are hopeful but will have to be confirmed with 3D reference calculations with an implemented version of the model in the solver AVL Fire.

Acknowledgements

This work is partly sponsored by PSA Peugeot Citroen and AVL. This support is gratefully acknowledged by the authors.

References

[1] A. Andriotis, M. Gavaises, and C. Arcoumanis. Vortex flow and cavitation in diesel injector nozzles. *Journal of Fluid Mechanics*, 610(-1):195–215, 2008.

[2] G. Blokkeel, R. Borghi, and Barbeau B. A 3d eulerian model to improve the primary breakup of atomizing jet. *SAE Technical Papers*, 2003. 2003-01-00005.

[3] F.X. Demoulin, P.A. Beau, G. Blokkeel, A. Mura, and R. Borghi. A new model for turbulent flows with large density fluctuations: application to liquid atomization. *Atom. and Sprays*, 17:315–345, 2007.

[4] J.P. Franc. The rayleigh-plesset equation: a simple and powerful tool to understand various aspects of cavitation. *In Fluid Dynamics of Cavitation and Cavitating Turbopumps, CISM Courses and Lectures*, 496, 2007.

[5] Lu He and Francisco Ruiz. Effect of cavitation on flow and turbulence in plain orifices for high-speed atomization. *Atomization and Sprays*, 5(6):569–584, 1995.

[6] R. Lebas, T. Menard, P.A. Beau, A. Berlemont, and F.X. Demoulin. Numerical simulation of primary breakup and atomization: Dns and modelling study. *International Journal of Multiphase Flow*, 35(3):247 – 260, 2008.

[7] F.E. Marble and J.E. Broadwell. The coherent flame model for turbulent chemical reactions. Technical report, Purdue University, West Lafayette, IN, 1977.

[8] F. Payri, V. Bermudez, R. Payri, and F. J. Salvador. The influence of cavitation on the internal flow and the spray characteristics in diesel injection nozzles. *Fuel*, 83(4-5):419 – 431, 2004.

[9] N. Tamaki, M. Shimizu, and H. Hiroyasu. Enhancement of the atomization of a liquid jet by cavitation in the nozzle hole. *Atomization and Sprays*, 11(2):2–14, 2001.

[10] A. Vallet and R. Borghi. Modelisation eulerienne de l'atomisation d'un jet liquide. *C. R. Acad. Sci. Paris*, Ser. II b 327:1015–1020, 1999.

[11] A. Vallet, A.A. Burluka, and R. Borghi. Development of an eulerian model for the atomization of a liquid jet. *Atomization and Sprays*, 11:619 – 642, 2001.